



1 **Preparation of TFC Membranes Supported with Elelctrospun Nanofibers** 2 **for Desalination by Forward Osmosis**

3 Mustafa Al-Furaiji^{1,*}, Mohammed Kadhom², Khairi Kalash¹, Basma Waisi³, and Noor Albayati⁴

4 ¹ Environment and Water Directorate, Ministry of Science and Technology, Baghdad, Iraq

5 ² Department of Environment, College of Energy and Environmental Sciences, Alkarkh University of Science, Baghdad, Iraq

6 ³ Department of Chemical Engineering, College of Engineering, University of Baghdad, Baghdad, Iraq

7 ⁴ Department of Science, College of Basic Education, University of Wasit, Azizia, Wasit, Iraq

8 Corresponding Author: email: alfuraiji79@gmail.com; phone: +964-7736-792-156

9 **Abstract**

10 Forward osmosis (FO) process has been considered as a viable option for water desalination in
11 comparison to the traditional processes like reverse osmosis regarding the energy consumption and
12 economical operation. In this work, polyacrylonitrile (PAN) nanofiber support layer was prepared using
13 electrospinning process as a modern method. Then, an interfacial polymerization reaction between m-
14 phenylenediamine (MPD) and trimesoyl chloride (TMC) was carried out to generate a polyamide
15 selective thin film composite (TFC) membrane on the support layer. The TFC membrane was tested in
16 FO mode (feed solution facing the active layer) using standard methodology and compared to a
17 commercially available cellulose triacetate membrane (CTA). The synthesized membrane showed a high
18 performance in terms of water flux ($16 \text{ Lm}^{-2}\text{h}^{-1}$) but traded the salt rejection ($4 \text{ gm}^{-2}\text{h}^{-1}$) comparing with
19 the commercially CTA membrane (water flux= $13 \text{ Lm}^{-2}\text{h}^{-1}$ and salt rejection= $3 \text{ gm}^{-2}\text{h}^{-1}$) at no applied
20 pressure and room temperature. Scanning electron microscopy (SEM), contact angle, mechanical
21 properties, porosity, and performance characterizations were conducted to examine the membrane.

22

23 **Keywords: Forward Osmosis; TFC membrane; Desalination; Nanofibers; Electrospinning**

24



25 **1. Introduction**

26 Forward osmosis (FO) is an osmotically driven membrane process which uses the difference in osmotic
27 pressure between the feed solution and a highly concentrated solution (called draw solution) to drive the
28 pure water from feed solution through the membrane to the draw solution. The FO process has many
29 advantages over other types of filtration processes such as its low or no trans-pressure, very high rejection
30 for various contaminants, low membrane fouling tendency than other filtration processes, and easy
31 building and operating equipment used is very simple and membrane support is less of a problem (Al-
32 Furajji et al., 2018; Cath et al., 2006).

33 One of the crucial aspects of developing FO process is making a suitable membrane for this process. The
34 ideal membrane has to be highly porous, thin, with good mechanical properties and provides high
35 rejection of salts and impurities (Ang et al., 2019). Thin-film composite (TFC) membranes have been
36 widely used in reverse osmosis studies and proven to have excellent performance in desalination (Kadhom
37 et al., 2016; Kadhom and Deng, 2018). However, recently TFC membranes have attracted more attention
38 in FO applications.

39 Commonly, the TFC membranes consist of two layers: a thin selective film that permits water molecules
40 to pass through but seize salts and other contaminations and a support layer that provides the required
41 mechanical properties (Ren and McCutcheon, 2014). The selective thin layer is typically prepared by
42 interfacial polymerization reaction of m-phenylenediamine (MPD) aqueous solution and 1,3,5-
43 Benzenetricarbonyl trichloride, which is familiarly called trimesoyl chloride (TMC), organic solution on
44 the support layer. The support sheet is conventionally prepared by phase inversion casting method. Here,
45 we adopted an emerging technology, electrospinning, to make the support layer. Electrospinning has some
46 advantages over the traditional phase inversion technique that include producing highly porous layer and
47 generating sub-micron fibers with highly controllable properties (Waisi et al., 2019). These properties
48 have led to introduce these nanofiber sheets as promising alternatives for the conventional FO membrane
49 support layers. Bui and McCutcheon 2013 investigated blending two kinds of polymer (i.e. PAN and
50 cellulose acetate) to make hydrophilic nanofibers for FO applications (Bui and McCutcheon, 2013).
51 Huang and McCutcheon 2014 used Nylon 6,6 electrospun nanofibers as support for TFC FO membranes



52 (Huang and McCutcheon, 2014). Chowdhury et al. 2016 prepared and tested a TFC membrane supported
53 with commercial polyethersulfone (PES) nanofiber membranes (Chowdhury et al., 2017). All these
54 electrospun nanofiber based TFC membrane showed excellent performance over the commercially
55 available FO membranes.

56 In this work, thin film composite polyamide membrane was synthesized by reacting the MPD and TMC
57 on the electrospun PAN nanofibers support layer and was utilized in the forward osmosis process. The
58 membranes prepared in this study were mainly characterized by SEM and contact angle to investigate the
59 impact of the highly porous support layer, in addition to other tests. FO experiments were carried out
60 using a custom-built setup using sodium chloride as a draw solution for the process.

61 **2. Materials and Methods**

62 **2.1. Materials**

63 Polyacrylonitrile (PAN) of an average molecular weight of 150,000 was purchased from Macklin,
64 Shanghai, China. N, Ndimethylformamide (DMF) and Isooctane were obtained from Fluka Chemie
65 AG, Buchs, Switzerland. The interfacial polymerization raw materials (*m*-phenylenediamine (>99%) and
66 trimesoyl chloride (98%)) were ordered from Merck. Sodium chloride (NaCl) was purchased from
67 Thomas Baker, India. Polyethersulfone (PES) of a M.wt. = 150,000 was purchased from Macklin
68 (Shanghai, China).

69 The control membrane used in this work was CTA (cellulose triacetate) forward osmosis membrane. This
70 membrane was provided by Hydration Technology Innovations (HTI) Water Technology (Albany, OR)
71 and been widely applied for a number of FO applications such as seawater desalination (Linares et al.,
72 2017), wastewater treatment (Al-Furaiji et al., 2019), and advanced life support systems (Cath et al.,
73 2005). Properties and images of the membrane can be found elsewhere (McCutcheon et al., 2005).

74 **2.2. PAN nanofiber and PES support layers fabrication**

75 PAN nanofibers were prepared using a custom-built electrospinning setup (Figure 1). The electrospinning
76 setup contained a high voltage power supply, syringe pump, and a rotating drum. Syringe pump was made
77 from locally available materials. A grounded aluminum rotating drum, which served as a collector, was



78 placed on a distance of 15 cm from the needle's tip, and an electrical potential was used at a voltage of
79 30 kV using the power supply device.

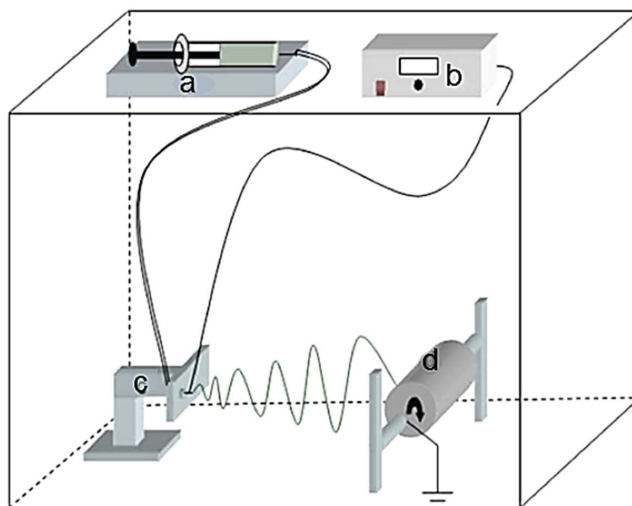
80

81 Solution of PAN in DMF was prepared by continuously stirring the polymer in the solvent for 24 h at
82 60°C. After obtaining the desired solution, it was left to cool and degas overnight at room temperature
83 prior to electrospinning. The as-prepared polymeric solution was electrospun at flowrate of 1 mL/h onto
84 an aluminum foil which is peeled off before using the membrane in preparing the TFC membranes.
85 Electrospinning was conducted at ambient temperature and humidity.

86 In order to compare the mechanical properties of the prepared support layer with a common
87 support layer used for the same purpose, a polyethersulfone support sheet was prepared via the phase
88 inversion phenomenon. 15% PES was dissolved in DMF by applying heat and stirring for 3 h until
89 colorless solution formed without any polymer residue. After maintaining the solution at 60 °C during
90 heating, it was left to cool at room temperature overnight for degassing. The solution was extended on a
91 glass plate via a home-made casting knife to a thickness of 130 μm and immersed in a water bath. The
92 solution turned to a white sheet and separated from the glass in few seconds. The sheet was rinsed with
93 water three times before storing and use.



94



95

96 **Figure 1 Photograph of the custom-built Electrospinning setup, (a) syringe pump, (b) high voltage supply, (c)**
97 **transition stage, and (d) rotating collector.**

98

99 **2.3. Interfacial Polymerization to Make TFC Membrane.**

100 The TFC membranes were prepared via interfacial polymerization reaction at the interface between MPD
101 aqueous solution and TMC organic solution. 2% of MPD was dissolved in DI water to prepare the
102 aqueous solution, while the organic solution was prepared by dissolving 0.15% of TMC in isooctane. The
103 IP reaction was conducted on the PAN support layer as follows: First, the as spun PAN was mounted on
104 a glass plate and the MPD solution poured on its top and kept in contact with the PAN support sheet for
105 60 s (Kadhom et al., 2016). The excess of the solution was ejected using a squeegee ruler. Then, the TMC
106 solution was poured on the PAN sheet that contains the MPD active sites and kept in contact for 30 s. The
107 resulting TFC membrane was then dried for 10 min at 60 °C and stored in DI water prior to the
108 performance examination.

109

110



111 **2.4. Membranes Characterizations**

112 The Morphology analysis of the prepared membranes was determined using Scanning Electron
113 Microscope (SEM, VEGA3 - TESCAN, Czechoslovakia). The mechanical properties of the different
114 membranes were obtained from the tensile tests in air at 25 °C using an Instron microforce tester. A
115 dynamic mechanical analysis (DMA) controlled force module was selected and a minimum of three strips
116 (with a size of 40 mm x 5.5 mm) were tested from each type of membrane. Porosity of the membranes
117 was estimated using gravimetric method. The membrane was cut as disks with diameter of 2.54 cm (1
118 in) and weighed (W_{dry}). Isopropyl alcohol (IPA) was used as a wetting agent and the membrane weighed
119 after immersed in IPA (W_{wet}). The porosity (ε) was calculated from the following equation:

$$120 \quad \varepsilon = \frac{\left(\frac{W_{wet} - W_{dry}}{\rho_{IPA}} \right)}{V} \times 100\%$$

121 where ρ_{IPA} is the density of IPA and V is the total volume of the sample. Each membrane were tested at
122 least three times. Wettability of the membranes was studied by measuring the contact angle (Theta Lite
123 TL-101 Thailand).

124 **2.5. Forward osmosis performance tests**

125 The FO tests were carried out using the experimental set-up illustrated in Figure 2. The installation
126 consists of two tanks: one was specified for the feed solution, while the other was assigned for the draw
127 solution. Both solutions were pumped to the membrane cell using diaphragm pumps from Pure-water®.
128 The membrane was installed in a custom-made cell with dimensions of 3"length, 1"width, and 1/8"depth.
129 The selection of the feed solution and draw solution was according to the standard methodology that was
130 described by Cath et al. 2013. The DI water was used as feed solution while 1 M NaCl solution was used
131 as draw solution. The water permeation flux was estimated as follows:

$$132 \quad J_w = \frac{\Delta w}{\rho A t}$$

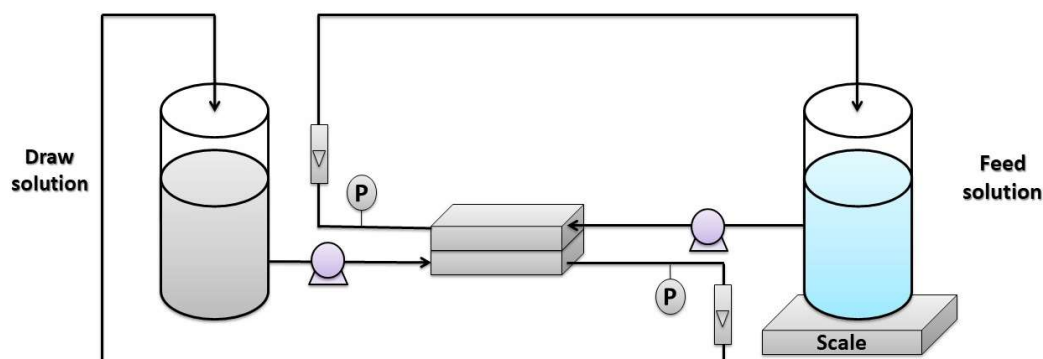
133 Where J_w is the water flux ($\text{Lm}^{-2}\text{h}^{-1}$), Δw represents the difference in the feed solution weight (g), ρ is
134 water density at operating temperature (g/L), A is the actual operative area of the membrane (20×10^{-4}
135 m^2), and t is the experiment's time.



136 Solute flux through the membrane was estimated by monitoring the conductivity of the feed solution and
137 using the following equation:

$$138 \quad J_s = \frac{\Delta CV}{At}$$

139 Where J_s represents the solute flux ($\text{gm}^{-2}\text{h}^{-1}$), ΔC is the change in the feed solution concentration (g/L)
140 (calculated from the conductivity change), and V stands for the volume of feed solution (L).



141

142

Figure 2 Schematic diagram of the FO bench-scale test unit.

143 3. Results and Discussion

144 3.1. Membrane characterization

145 Figure 3 illustrates the SEM captures of the PAN support layer that was prepared by electrospinning
146 technique. It can be observed that the membrane structured of smooth and uniform fibers with
147 approximate diameter of 250 nm. Cross-sectional SEM image (Figure 4) shows that the membrane
148 consists of nanofibrous layers with a thickness of about 75 microns. It can also be noticed that the
149 underlying nanofibers owns a very high porosity on their surfaces. This could assure maximum contact
150 between PAN nanofibers with the draw solution during the forward osmosis operation, which means
151 higher mass transfer area and consequently higher water flux. Figure 5 illustrates the surface morphology
152 of the PAN nanofiber membrane after the interfacial polymerization reaction. Also, it can be seen that
153 polyamide selective membrane was successfully formed on the PAN nanofiber support sheet. Contact



154 angle measurement of the prepared membranes showed that it has extremely hydrophilic surface with
155 average contact angle of 35° (Figure 6). Hydrophilicity of membrane's surface is an important factor in
156 the osmotically driven membrane processes (Darwish et al., 2020). This could be explained as the solutes
157 can exclusively diffuse within the wetted area of the support sheet. Ultimately, the unsaturated parts inside
158 the internal structure of the support layer couldn't be calculated as an actual mass transfer area. As much
159 as the internal surfaces of the pores and inner vacancy get wet, the porous support layer can contribute to
160 produce a membrane with a better osmotic water flux performance.

161 **3.2. Support sheet mechanical properties and porosity**

162 3.2.1 Mechanical properties

163 Using a support layer for the TFC membrane that usually applied in nanofiltration, reverse
164 osmosis, and forward osmosis is inevitable due to the tiny thickness of the active membrane. The support
165 layer was found to significantly affect the total performance and commonly made of polymers. Many
166 factors could influence the layer usage such as its raw material, method and conditions of preparation,
167 doping additives, porosity, tortuosity, etc (Kadhom and Deng, 2018). In most cases, the support layer is
168 manufactured using the phase inversion phenomenon for a low hydrophilicity polymer. In this work, a
169 PAN layer was synthesized using the electrospinning, which is expected to produce higher internal
170 porosity than the sheets produced via phase inversion. Therefore, the mechanical properties were studied
171 and compared to the commonly used support layer that produced by phase inversion.

172 Figure 7 shows the relation between the stress and strain of the PAN sheet. It can observe that the
173 maximum stress was 1.258 MPa, which was associated with a strain of 15.31%. When these values were
174 compared with 15% Polyethersulfone support sheet (as an example of the familiarly applied support
175 layers), the stress is lower but the strain is higher. The measured stress and strain of the PES sheet were
176 around 2.45 MPa and 8.7%, respectively. It can be noted that the PAN sheets had a lower mechanical
177 strength but higher elongation rate. This result is expected due to the method of preparation, where in the
178 electrospinning the nanofibers are made individually and connect with each other on the rotating cylinder.
179 While in the phase inversion, the sheet formed by stiffening the polymer and discarding the solvent. The



180 average values of other mechanical properties were listed in Table 1 with the standard deviation of three
181 measurement values.

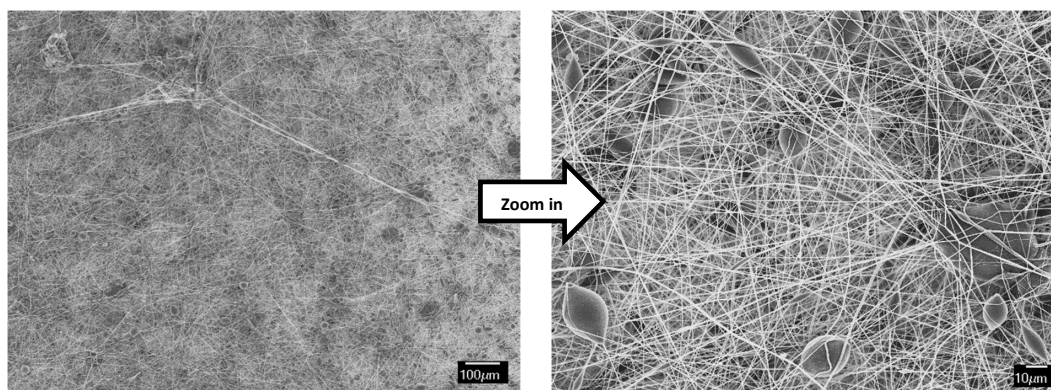
182 **Table 1. Mechanical properties of PAN support layer**

| Mechanical Property | Average value | Standard deviation | Units |
|---------------------|---------------|--------------------|-------|
| Young's modulus | 9.4065 | 1.0288 | MPa |
| Tensile strength | 1.3586 | 0.1428 | MPa |
| Elongation at break | 17.8463 | 3.5857 | (%) |

183

184 3.2.2 Porosity

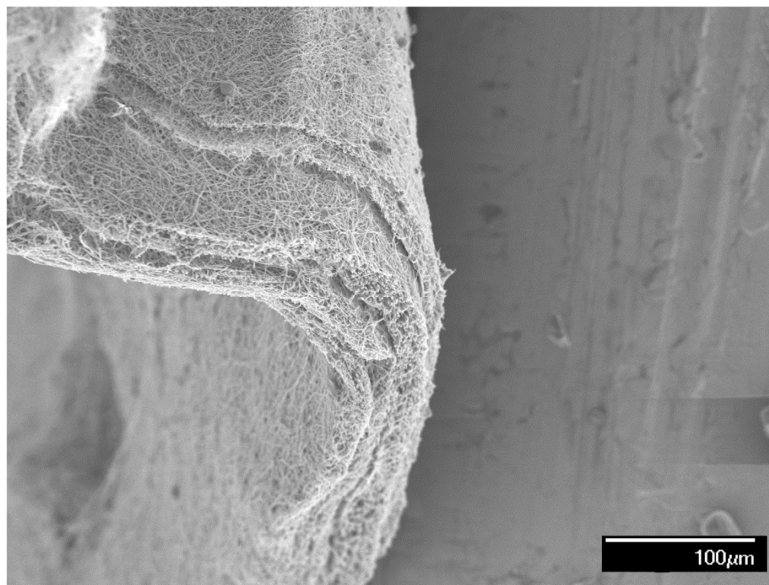
185 PAN support layer was prepared by the electrospinning to achieve a high porosity. However, the
186 average porosity values of the PAN and classic PES layers were $92.07\% \pm 2.09$ and $60.0\% \pm 1.53$,
187 respectively. From these values, it can be seen that the PAN sheet is more porous than the PES sheet.
188 This could help in penetrating the water and, anyway, solute through the membrane structure, which could
189 improve the water flux. Higher porosity means lower unreachable spaces and dead ends.



190

191 **Figure 3 Surface SEM images of the as-spun PAN nanofiber mat.**

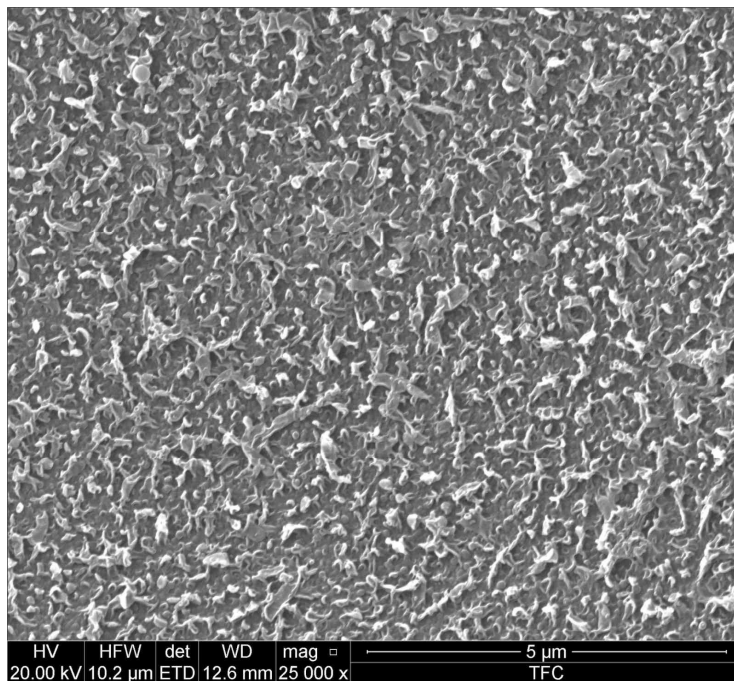
192



193

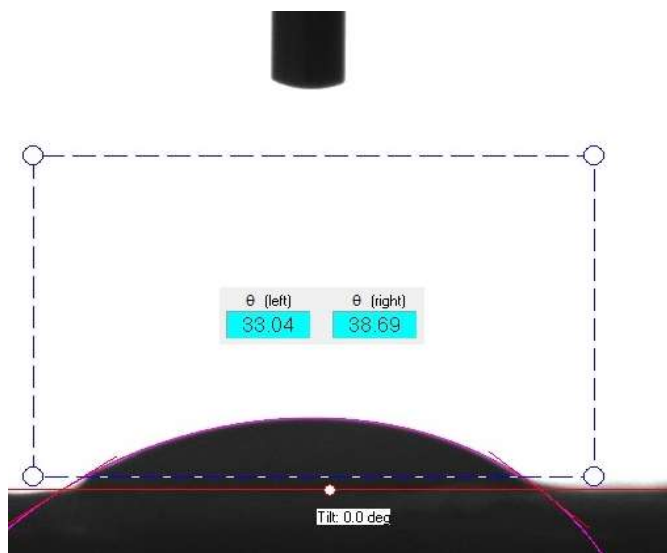
194

Figure 4 Cross-sectional SEM image of the as-spun PAN nanofiber mat.



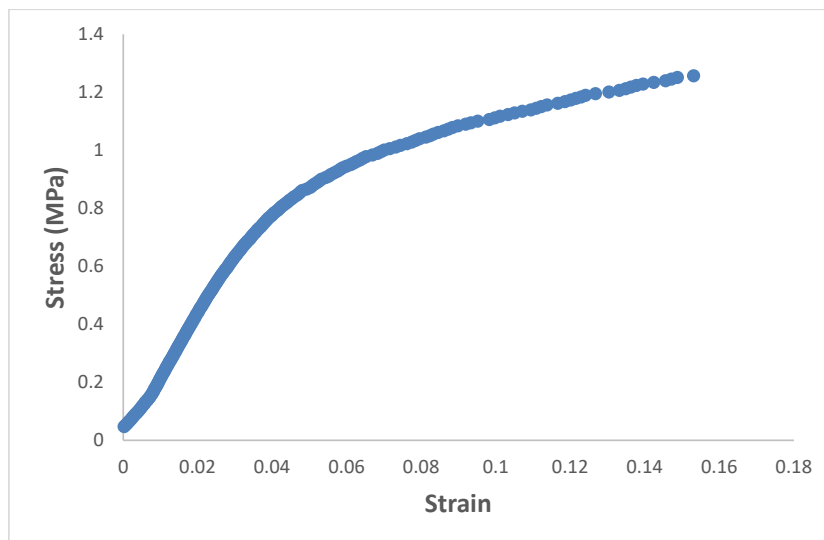
195

Figure 5 Surface SEM image of the TFC PAN membrane.



196

Figure 6 Contact angle of the PAN nanofiber membrane.



197

198

Figure 7 Stress and strain relationship of PAN support layer

199

3.3. Membrane performance in FO operation

200

201

202

203

204

205

206

207

208

209

210

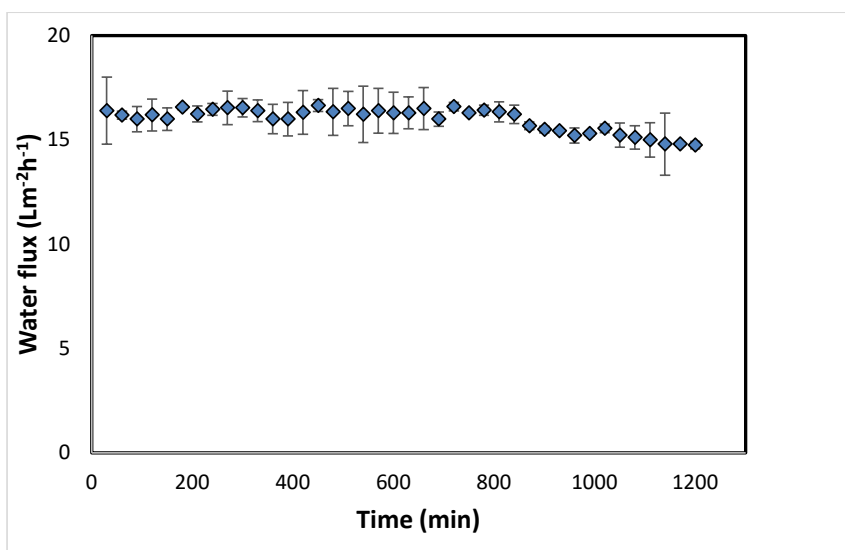
211

212

The osmotic efficiency of the TFC membrane supported by nanofiber layer was examined using DI water as feed solution, whereas 1 M NaCl solution was used as draw solution according to the standard methodology for testing the osmotically driven membranes (Cath et al., 2013). Results of water flux and salt reverse flux are clarified in Figures 8 and 9, respectively. PAN-TFC membrane showed stable flux of about 16 LMH for 20 h of operation. Reverse salt flux exhibited similar behavior with average value of about 4 GMH. In order to comparing the performance of the PAN-TFC membrane with commercial membranes, we tested CTA membranes from HTI under the same operating conditions, the results were illustrated in Figure 10. It can be distinguished from the figure that the PAN-TFC membrane's water flux was higher than the HTI-CTA membrane's water flux. This could be attributed to the highly porous surface structure of the nanofiber support layer for PAN-TFC membrane; this porous surface generates more affective mass transfer area, and consequently higher water flux. However, the reverse salt flux of the commercial membrane was lower compared to the PAN-TFC membrane. This could ascribe to its better mechanical strength and rigidity comparing with the nanofibrous composite membranes, which

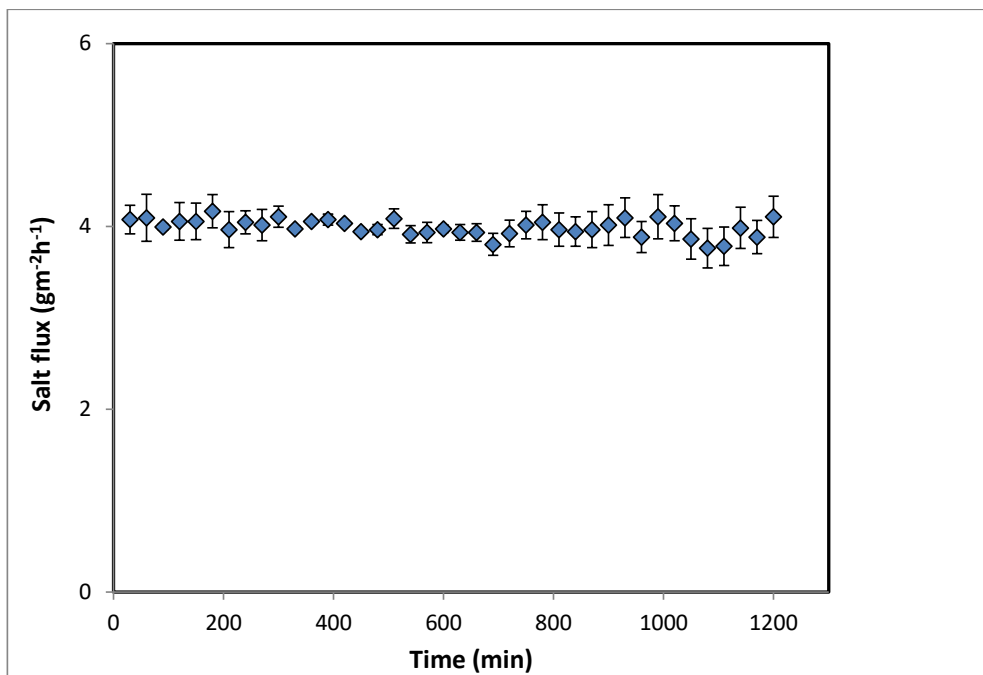


213 are commonly have modest mechanical properties. Nevertheless, the FO applications are famous to have
214 low or no hydraulic pressure required to drive the process; here, it can be resulted that the osmotic
215 efficiency of the membrane is more important than its rigidity.



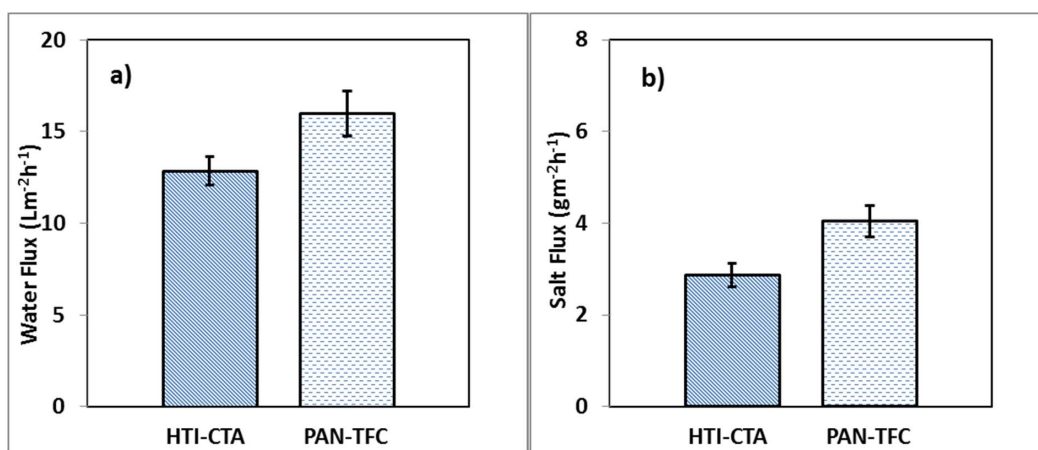
216

217 **Figure 8 Forward osmosis water flux for the PAN-TFC membrane. Experimental conditions: feed solution: DI water,**
218 **draw solution: 1 M NaCl, FO mode, volumetric flow-rate of feed and draw 0.6 L/min, Temp 25° C, zero transmembrane**
219 **pressure. Results are an average of three experiments with different coupons. Error bars indicate standard deviation.**



220

221 **Figure 9** Forward osmosis salt flux for the PAN-TFC membrane. Experimental conditions: feed solution: DI water,
222 draw solution: 1 M NaCl, FO mode, volumetric flow-rate of feed and draw 0.6 L/min, Temp 25° C, zero transmembrane
223 pressure. Results are an average of three experiments with different coupons. Error bars indicate standard deviation.



224



225 **Figure 10 Forward osmosis water flux and salt flux for the PAN-TFC membrane. Experimental conditions: feed**
226 **solution: DI water, draw solution: 1 M NaCl, FO mode, volumetric flow-rate of feed and draw 0.6 L/min, Temp 25° C,**
227 **zero transmembrane pressure. Results are an average of three experiments with different coupons. Error bars indicate**
228 **standard deviation.**

229 **4. Conclusions and Recommendations**

230 TFC membrane with fibrous structure was prepared in this research and tested for forward osmosis
231 application. Electrospinning setup was made from locally available parts. This system exhibited stable
232 operation in making the electrospun nanofiber membrane. The prepared TFC membrane showed good
233 performance in terms of water flux and salt rejection. TFC-PAN membranes showed a stable water flux
234 with an average value of 16 LMH comparing to the CTA commercial membranes with 13 LMH water
235 flux. Future research can focus in incorporating specific nanoparticles to enhance membranes'
236 performance. Also, studying exposure time of MPD and TMC on the performance of the membrane is
237 highly recommended.

238

239

240

241

242

243

244

245



246 References

- 247 Al-Furaiji, M., Benes, N., Nijmeijer, A., McCutcheon, J.R., 2019. Use of a Forward Osmosis-
248 Membrane Distillation Integrated Process in the Treatment of High-Salinity Oily Wastewater. *Ind.*
249 *Eng. Chem. Res.* 58, 956–962. <https://doi.org/10.1021/acs.iecr.8b04875>
- 250 Al-Furaiji, M.H.O., Arena, J.T., Chowdhury, M., Benes, N., Nijmeijer, A., McCutcheon, J.R., 2018.
251 Use of forward osmosis in treatment of hyper-saline water. *Desalin. WATER Treat.* 133, 1–9.
252 <https://doi.org/10.5004/dwt.2018.22851>
- 253 Ang, W.L., Wahab Mohammad, A., Johnson, D., Hilal, N., 2019. Forward osmosis research trends in
254 desalination and wastewater treatment: A review of research trends over the past decade. *J. Water*
255 *Process Eng.* 31, 100886. <https://doi.org/10.1016/j.jwpe.2019.100886>
- 256 Bui, N.N., McCutcheon, J.R., 2013. Hydrophilic nanofibers as new supports for thin film composite
257 membranes for engineered osmosis. *Environ. Sci. Technol.* 47, 1761–1769.
258 <https://doi.org/10.1021/es304215g>
- 259 Cath, T.Y., Adams, D., Childress, A.E., 2005. Membrane contactor processes for wastewater
260 reclamation in space: II. Combined direct osmosis, osmotic distillation, and membrane distillation
261 for treatment of metabolic wastewater. *J. Memb. Sci.* 257, 111–119.
262 <https://doi.org/10.1016/j.memsci.2004.07.039>
- 263 Cath, T.Y., Childress, A.E., Elimelech, M., 2006. Forward osmosis: Principles, applications, and recent
264 developments. *J. Memb. Sci.* 281, 70–87. <https://doi.org/10.1016/j.memsci.2006.05.048>
- 265 Cath, T.Y., Elimelech, M., McCutcheon, J.R., McGinnis, R.L., Achilli, A., Anastasio, D., Brady, A.R.,
266 Childress, A.E., Farr, I. V., Hancock, N.T., Lampi, J., Nghiem, L.D., Xie, M., Yip, N.Y., 2013.
267 Standard Methodology for Evaluating Membrane Performance in Osmotically Driven Membrane
268 Processes. *Desalination* 312, 31–38. <https://doi.org/10.1016/j.desal.2012.07.005>
- 269 Chowdhury, M.R., Huang, L., McCutcheon, J.R., 2017. Thin Film Composite Membranes for Forward
270 Osmosis Supported by Commercial Nanofiber Nonwovens. *Ind. Eng. Chem. Res.* 56, 1057–1063.
271 <https://doi.org/10.1021/acs.iecr.6b04256>
- 272 Darwish, N. Bin, Alkudhiri, A., AlRomaih, H., Alalawi, A., Leaper, M.C., Hilal, N., 2020. Effect of
273 lithium chloride additive on forward osmosis membranes performance. *J. Water Process Eng.* 33,



- 274 101049. <https://doi.org/10.1016/j.jwpe.2019.101049>
- 275 Huang, L., McCutcheon, J.R., 2014. Hydrophilic nylon 6,6 nanofibers supported thin film composite
276 membranes for engineered osmosis. *J. Memb. Sci.* 457, 162–169.
277 <https://doi.org/10.1016/j.memsci.2014.01.040>
- 278 Kadhom, M., Deng, B., 2018. Synthesis of high-performance thin film composite (TFC) membranes by
279 controlling the preparation conditions: Technical notes. *J. Water Process Eng.*
280 <https://doi.org/10.1016/j.jwpe.2017.12.011>
- 281 Kadhom, M., Yin, J., Deng, B., 2016. A Thin Film Nanocomposite Membrane with MCM-41 Silica
282 Nanoparticles for Brackish Water Purification. <https://doi.org/10.3390/membranes6040050>
- 283 Linares, R.V., Li, Z., Elimelech, M., Amy, G., Vrouwenvelder, H., 2017. Recent Developments in
284 Forward Osmosis Processes. *Water Intell. Online.* <https://doi.org/10.2166/9781780408125>
- 285 McCutcheon, J.R., McGinnis, R.L., Elimelech, M., 2005. A novel ammonia-carbon dioxide forward
286 (direct) osmosis desalination process. *Desalination* 174, 1–11.
287 <https://doi.org/10.1016/j.desal.2004.11.002>
- 288 Ren, J., McCutcheon, J.R., 2014. A new commercial thin film composite membrane for forward
289 osmosis. *Desalination* 343, 187–193. <https://doi.org/10.1016/j.desal.2013.11.026>
- 290 Waisi, B.I., Manickam, S.S., Benes, N.E., Nijmeijer, A., McCutcheon, J.R., 2019. Activated Carbon
291 Nanofiber Nonwovens: Improving Strength and Surface Area by Tuning Fabrication Procedure.
292 *Ind. Eng. Chem. Res.* 58, 4084–4089. <https://doi.org/10.1021/acs.iecr.8b05612>
- 293
- 294